

Representation Theorems for an Infinite Shear Fault*

Robert J. Geller

(Received May 1 1974)

Summary

The Green's function solutions for a shear dislocation with symmetry in the direction of infinite length have been integrated analytically over the direction of infinite length. The displacement solution is reduced from a surface integral over the fault plane to a line integral of temporal convolutions over the width of the fault. If the time history function of fault displacement is any piecewise linear function the convolutions can be integrated analytically, reducing the solutions to line integrals. Numerical results and plots are presented for a simple example. The two-dimensional solutions give exact first motions at points 'over' the fault. Also the solutions can be used to test two-dimensional finite difference and finite element computer programs.

1. Introduction

Although the general Green's function solutions for displacements in an elastic body have been known formally for many years (e.g. de Hoop 1958), the solutions were not presented in a form suited to computation until interest grew in numerical modelling of near field effects. Maruyama (1963) demonstrated that displacements from dynamic dislocation are equivalent to displacements caused by time varying double couples. Haskell (1964) showed that double couples corresponded to only one of the terms of de Hoop's representation theorem.

Haskell (1969) presented general surface integral representations for the displacement caused by a shear dislocation. Haskell & Thomson (1972) presented similar representations for the displacement caused by a tensile (or compressive) dislocation. Thomson & Haskell (1972) presented numerical results for transverse shear dislocations. The numerical results accompanying the 1969 paper were computed for the much simpler cases of piecewise linear time functions with infinite rupture velocity along the length† of the fault plane. In effect Haskell's model differed from a completely two-dimensional treatment only in that his fault had finite length.

Haskell's (1969) solutions are exactly equivalent to the two-dimensional case until waves from the edge reach a point at which one is computing displacements. (If a point does not lie in the cylinder defined by the fault length the first arrival at that point is from the edge.) Thus a two-dimensional treatment will give exact first motion solutions at any point 'above' the fault. Another use for analytic solutions for two-dimensional shear dislocation problems is in testing two-dimensional finite element and finite difference computer programs.

* Division of Geological and Planetary Sciences, Contribution No. 2456.

† In this paper length is along the x_2 axis; width along the x_1 axis.

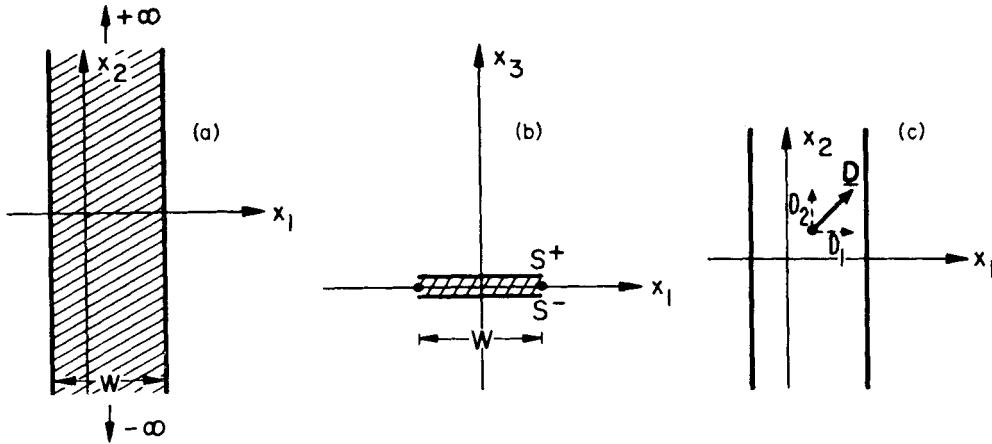


FIG. 1. Fault model used in this paper. D is the slip vector.

Two-dimensional dislocation solutions are effectively the result of adding up line sources. Although it has long been known that the two-dimensional Green's function could formally be derived by integrating the three-dimensional Green's function from $-\infty$ to $+\infty$, the integral has not been explicitly evaluated. The derivation of the explicit two-dimensional solutions is the subject of the next section.

2. Two-dimensional dislocation fault models

The fault model used in this paper is shown in Fig. 1. We will calculate the displacement solutions for a fault in an isotropic homogeneous whole space with infinite length in the x_2 direction (from $-\infty$ to $+\infty$) and no geometrical or functional dependence on x_2 . (i.e. all planes perpendicular to the x_2 axis are exactly identical at any fixed time.)

Notation

S	= Bounding surface of linearly elastic region, consisting of a surface at $R = \infty$ and the surface enclosing the (non-linear) fault zone.
S^+	= Bounding surface above (x_3 intercept > 0) the fault zone.
\mathbf{n}^+	= Unit normal outward from S^+ into non-linear zone. = $(0, 0, -1)$ for the fault model in Fig. 1.
W	= A line on S^+ perpendicular to the x_2 axis, traversing the fault surface.
$\mathbf{u} = (u_1, u_2, u_3)$	= Displacement vector at any point.
$\mathbf{x} = (x_1, x_2, x_3)$	= Co-ordinates of a point at which displacement will be evaluated.
$\xi = (\xi_1, \xi_2, \xi_3)$	= Co-ordinates of points on S^+ .
ρ	= Density.
λ, μ	= Lamé's constants.

- $\alpha = \sqrt{\left(\frac{\lambda + 2\mu}{\rho}\right)}$ = Compressional velocity.
 $\beta = \sqrt{\left(\frac{\mu}{\rho}\right)}$ = Shear velocity.
 δ_{ij} = Kronecker delta.
 $C_{j k p q} = \lambda \delta_{j k} \delta_{p q} + \mu \delta_{j p} \delta_{k q} + \mu \delta_{j q} \delta_{k p}$
 $H(t)$ = Heaviside step function.
 $a(t) * b(t) = \int_0^t a(t-\tau) b(\tau) d\tau$ = Convolution.
 i, j, k = Latin subscripts take values of 1, 2 and 3.
 ν, δ, ε = Greek subscripts take values of 1 and 3 only.
 G_{ij} = The (three-dimensional) Green's tensor operator.
 $G_{ij, k} = \frac{\partial G_{ij}}{\partial x_k}$ = Spatial derivative of Green's tensor operator.
 $\dot{\phi}(\xi, t) = \frac{\partial \phi(\xi, t)}{\partial t}$ = Time derivative of a function.
 $R = |\mathbf{x} - \xi| = \sqrt{(x_1 - \xi_1)^2 + (x_2 - \xi_2)^2 + (x_3 - \xi_3)^2}$
 $r = \sqrt{(x_1 - \xi_1)^2 + (x_3 - \xi_3)^2}$
 $\omega_i = \frac{x_i - \xi_i}{R}$ = Three-dimensional direction cosine.
 $\gamma_z = \frac{x_z - \xi_z}{r}$ = Two-dimensional direction cosine.
 $\mathbf{D}(\xi, t) = \mathbf{u}^+ - \mathbf{u}^-$ = Dislocation across the fault.

The convention of summation over repeated dummy indices is used throughout.

The Green's function operator was shown to be

$$G_{ij}(\phi(\xi, t)) = \frac{1}{4\pi\rho} \left\{ \frac{\partial^2}{\partial x_i \partial x_j} \left[\frac{1}{R} \int_0^\infty \left(\phi(\xi, t - (R/\alpha) - t') - \phi(\xi, t - (R/\beta) - t') \right) t' dt' \right] + \frac{\phi(\xi, t - (R/\beta)) \delta_{ij}}{\beta^2 R} \right\} \quad (1a)$$

by de Hoop. Haskell used the equivalent, usually more convenient form

$$G_{ij}(\phi(\xi, t)) = \frac{1}{4\pi\rho} \left\{ \frac{3\omega_i \omega_j - \delta_{ij}}{R^3} \int_{R/\alpha}^{R/\beta} \phi(\xi, t - t') t' dt' + \frac{\omega_i \omega_j}{\alpha^2 R} \phi(\xi, t - (R/\alpha)) + \frac{\delta_{ij} - \omega_i \omega_j}{\beta^2 R} \phi(\xi, t - (R/\beta)) \right\} \quad (1b)$$

With no body forces in the linearly elastic region, and with tractions equal in magnitude and opposite in direction acting on S^+ and S^- the representation theorem of de Hoop, becomes (Haskell 1964)

$$u_i(\mathbf{x}, t) = \int_{S^+} \int C_{j k p q} G_{i p, q} [D_j(\xi, t)] n_k^+ dS. \quad (2)$$

(Even if the tractions are not equal and opposite while the dislocation is occurring, the thinness of the fault zone means that only very high frequencies will be affected.)

We will integrate out ξ_2 dependence to derive the two-dimensional Green's function derivative

$$\Gamma_{ij, k}(\phi(\xi_1, \xi_3, t)) = \int_{\xi_2=-\infty}^{\infty} G_{ij, k}(\phi(\xi_1, \xi_3, t)) d\xi_2. \quad (3)$$

For the remainder of the paper we will write functions as $\phi(\xi, t)$ with the implicit convention that no function has ξ_2 dependence. Further we assume that any function we deal with, $\phi(\xi, t) \equiv 0$, $t < 0$ and that there exists some positive τ such that $\phi(\xi, t)$ is constant, $t > \tau$. Also, since the solution is symmetric with respect to x_2 , we will evaluate all solutions at $x_2 = 0$ for algebraic convenience. Because of the symmetry of the two-dimensional problem

$$\Gamma_{2\alpha}(\phi(\xi, t)) = \Gamma_{22}(\phi(\xi, t)) \equiv 0. \quad (4)$$

Therefore, as one might expect, the equations decouple to give an 'SH' solution (for u_2) and a 'P-SV' solution (for u_1 and u_3).

Because there is no x_2 dependence:

$$4\pi\rho \Gamma_{22}(\phi(\xi, t)) = \int_{\xi_2=-\infty}^{\infty} \frac{\phi(\xi, t - (R/\beta))}{\beta^2 R} d\xi_2. \quad (5)$$

After differentiating and then integrating by parts, we find that

$$4\pi\rho \Gamma_{22, \eta}(\phi(\xi, t)) = -\frac{2\gamma_\eta}{\beta^3 r} \int_{\xi_2=0}^{\infty} \dot{\phi}(\xi, t - (R/\beta)) d\xi_2. \quad (6)$$

Take the Laplace transform of (6), giving

$$\Gamma_{22, \eta}(\bar{\phi}(\xi, s)) = -\frac{\gamma_\eta s}{2\pi\mu\beta r} \bar{\phi}(\xi, s) \int_{\xi_2=0}^{\infty} e^{-sR/\beta} d\xi_2. \quad (7)$$

Now use the Cagniard technique (Dix 1954) to rewrite (7) as

$$\Gamma_{22, \eta}(\bar{\phi}(\xi, s)) = -\frac{\gamma_\eta}{2\pi\mu r} s\bar{\phi}(\xi, s) \int_0^{\infty} e^{-st} \frac{tH(t-r/\beta)}{\sqrt{(t^2-r^2/\beta^2)}} dt. \quad (8)$$

The Laplace transform can be inverted by inspection to get a convolution (Churchill 1958)

$$\Gamma_{22, \eta}(\phi(\xi, t)) = -\frac{\gamma_\eta}{2\pi\mu r} \left[\phi(\xi, t) * \frac{tH(t-r/\beta)}{\sqrt{(t^2-r^2/\beta^2)}} \right]. \quad (9)$$

After some straightforward, but tedious, algebra along the same general lines, we find that the integral in (3) becomes

$$\begin{aligned} \Gamma_{\varepsilon\kappa, \eta}(\phi(\xi, t)) = & \frac{1}{2\pi\rho} \left\{ \left[(\phi(\xi, t)) \left(\frac{A-4B}{r^3} \right) \right] * \left[\frac{2t^2-r^2/\alpha^2}{\sqrt{(t^2-r^2/\alpha^2)}} H(t-r/\alpha) \right. \right. \\ & - \left. \frac{2t^2-r^2/\beta^2}{\sqrt{(t^2-r^2/\beta^2)}} H(t-r/\beta) \right] - \left[\frac{B\dot{\phi}(\xi, t)}{\alpha^2 r} \right] * \left[\frac{tH(t-r/\alpha)}{\sqrt{(t^2-r^2/\alpha^2)}} \right] \\ & + \left. \left[\frac{\dot{\phi}(\xi, t)}{\beta^2 r} * \frac{tH(t-r/\beta)}{\sqrt{(t^2-r^2/\beta^2)}} \right] [B-\gamma_\eta \delta_{\varepsilon\kappa}] \right\} \end{aligned} \quad (10a)$$

$$A = \delta_{\varepsilon\kappa} \gamma_\eta + \delta_{\varepsilon\eta} \gamma_\kappa + \delta_{\kappa\eta} \gamma_\varepsilon \quad (10b)$$

$$B = \gamma_\varepsilon \gamma_\kappa \gamma_\eta. \quad (10c)$$

Note that $\Gamma_{22, \eta}$ converges to the correct static solution

$$\lim_{t \rightarrow \infty} \Gamma_{22, \eta}(\phi(\xi, t)) = - \frac{\gamma_\eta \Phi(\xi)}{2\pi\mu r} \quad (11)$$

where $\Phi(\xi) = \lim_{t \rightarrow \infty} \phi(\xi, t)$.

Because none of the spatial derivatives associated with $\Gamma_{\varepsilon\kappa, \eta}(\phi(\xi, t))$ are zero (10a) should approach the general static solution as a limit. The general static solution is the Somigliana tensor (given in Love 1927, article 169, but in a different form).

$$m_{\varepsilon\kappa} \Phi = \frac{\Phi}{8\pi\mu} \left(\frac{\lambda+3\mu}{\lambda+2\mu} \cdot \frac{\delta_{\varepsilon\kappa}}{R} + \frac{\omega_\varepsilon \omega_\kappa}{R} \cdot \frac{\lambda+\mu}{\lambda+2\mu} \right). \quad (12)$$

If we define

$$M_{\varepsilon\kappa, \eta} \Phi = \int_{\xi_2 = -\infty}^{\infty} m_{\varepsilon\kappa, \eta} \Phi d\xi_2 \quad (13)$$

then

$$\begin{aligned} \lim_{t \rightarrow \infty} \Gamma_{\varepsilon\kappa, \eta} \Phi &= M_{\varepsilon\kappa, \eta} \Phi \\ &= \frac{\Phi}{4\pi\mu} \left\{ \left(\frac{\lambda+\mu}{\lambda+2\mu} A - 2\gamma_\eta \delta_{\varepsilon\kappa} \right) \cdot \frac{1}{r} - \frac{2(\lambda+\mu)B}{(\lambda+2\mu)r} \right\}. \end{aligned} \quad (14)$$

The solutions for displacements for the fault plane we have chosen are

$$u_2(\mathbf{x}, t) = \int_W -\mu \Gamma_{22, 3} [D_2(\xi, t)] dW \quad (15a)$$

$$u_\eta(\mathbf{x}, t) = \int_W -\mu (\Gamma_{\eta 1, 3} [D_1(\xi, t)] + \Gamma_{\eta 3, 1} [D_1(\xi, t)]) dW. \quad (15b)$$

Note that $G_{ij, k}$ as used in this paper is the negative of Haskell's $M_{ij, k}$. When written out explicitly, equations (15) become

$$\begin{aligned} u_1(\mathbf{x}, t) = & \frac{\beta^2}{2\pi} \int_W \left\{ \left(\frac{8\gamma_1^2 \gamma_3 - 2\gamma_3}{r^3} \right) [D_1(\xi, t)] * \left[\frac{2t^2-r^2/\alpha^2}{\sqrt{(t^2-r^2/\alpha^2)}} H(t-r/\alpha) \right. \right. \\ & - \left. \frac{2t^2-r^2/\beta^2}{\sqrt{(t^2-r^2/\beta^2)}} H(t-r/\beta) \right] + \left[\frac{2\gamma_1^2 \gamma_3 \dot{D}_1(\xi, t)}{\alpha^2 r} \right] * \left[\frac{tH(t-r/\alpha)}{\sqrt{(t^2-r^2/\alpha^2)}} \right] \\ & + \left. (\gamma_3 - 2\gamma_1^2 \gamma_3) \left[\frac{\dot{D}_1(\xi, t)}{\beta^2 r} \right] * \left[\frac{tH(t-r/\beta)}{\sqrt{(t^2-r^2/\beta^2)}} \right] \right\} dW \end{aligned} \quad (16a)$$

$$u_2(x, t) = \frac{1}{2\pi} \int_W \frac{\gamma_3}{r} [\dot{D}_2(\xi, t)] * \left[\frac{tH(t-r/\beta)}{\sqrt{(t^2-r^2/\beta^2)}} \right] dW \quad (16b)$$

$$\begin{aligned} u_3(x, t) = & \frac{\beta^2}{2\pi} \int_W \left\{ \left(\frac{8\gamma_1\gamma_3^2-2\gamma_1}{r^3} \right) [D_1(\xi, t)] * \left[\frac{2t^2-r^2/\alpha^2}{\sqrt{(t^2-r^2/\alpha^2)}} H(t-r/\alpha) \right. \right. \\ & - \left. \frac{2t^2-r^2/\beta^2}{\sqrt{(t^2-r^2/\beta^2)}} H\left(t-\frac{r}{\beta}\right) \right] + \left[\frac{2\gamma_1\gamma_3^2\dot{D}_1(\xi, t)}{\alpha^2 r} \right] * \left[\frac{tH(t-r/\alpha)}{\sqrt{(t^2-r^2/\alpha^2)}} \right] \\ & \left. + (\gamma_1-2\gamma_1\gamma_3^2) \left[\frac{\dot{D}_1(\xi, t)}{\beta^2 r} \right] * \left[\frac{tH(t-r/\beta)}{\sqrt{(t^2-r^2/\beta^2)}} \right] \right\} dW. \end{aligned} \quad (16c)$$

The integrands of equations (16a) and (16c) are equal to Niazy's (1973) U_H and W_H when D_1 is a step function in time.

3. Solutions when the time function is a ramp

The basic source time history function used by Haskell (1969) is a ramp.

$$D_i(\xi, t) = \begin{cases} 0 & t - \xi_1/v < 0 \\ (\Delta_i/T)(t - \xi_1/v) & 0 < t - \xi_1/v < T \\ \Delta_i & T < t - \xi_1/v \end{cases} \quad (17)$$

Δ_i is the final displacement offset, T is the rise time and v the rupture velocity, $\Delta_3 = 0$ for a shear fault.

The convolutions in equations (16) can be evaluated analytically for the time functions in (17). We will use c as a symbol which can represent either α or β in the two independent forms of the convolutions.

$$\begin{aligned} & [\dot{D}_i(\xi, t)] * \left[\frac{tH(t-r/c)}{\sqrt{(t^2-r^2/c^2)}} \right] \\ &= \begin{cases} 0 & t - \frac{r}{c} - \frac{\xi_1}{v} < 0 \\ \frac{\Delta_i}{T} \sqrt{\left(\left(t - \frac{\xi_1}{v} \right)^2 - \frac{r^2}{c^2} \right)} & 0 < t - \frac{r}{c} - \frac{\xi_1}{v} < T \\ \frac{\Delta_i}{T} \left(\sqrt{\left(\left(t - \frac{\xi_1}{v} \right)^2 - \frac{r^2}{c^2} \right)} - \sqrt{\left(\left(t - T - \frac{\xi_1}{v} \right)^2 - \frac{r^2}{c^2} \right)} \right) & T < t - \frac{r}{c} - \frac{\xi_1}{v} \end{cases} \end{aligned} \quad (18a)$$

$$D_i(\xi, t) * \left[\frac{2t^2 - r^2/c^2}{\sqrt{(t^2 - r^2/c^2)}} H\left(t - \frac{r}{c}\right) \right]$$

$$= \begin{cases} 0 & t - \frac{r}{c} - \frac{\xi_1}{v} < 0 \\ \frac{\Delta_i}{3T} \left[\left(\left(t - \frac{\xi_1}{v} \right)^2 - \frac{r^2}{c^2} \right)^{3/2} \right] & 0 < t - \frac{r}{c} - \frac{\xi_1}{v} < T \\ \frac{\Delta_i}{3T} \left[\left(\left(t - \frac{\xi_1}{v} \right)^2 - \frac{r^2}{c^2} \right)^{3/2} - \left(\left(t - \frac{\xi_1}{v} - T \right)^2 - \frac{r^2}{c^2} \right)^{3/2} \right] & T < t - \frac{r}{c} - \frac{\xi_1}{v}. \end{cases} \quad (18b)$$

Clearly the convolutions can be evaluated analytically for any piecewise linear source function. Therefore the dynamic solution for any source function can be approximated to any desired degree of accuracy.

The solutions in equations (16) were evaluated numerically for source functions of the type in (17). Parameters used were

$$\begin{aligned} \Delta_1 &= 100 \text{ cm} & v &= 2.3 \text{ km s}^{-1} \\ \Delta_2 &= 100 \text{ cm} & \alpha &= 6.0 \text{ km s}^{-1} \\ T &= 3.0 \text{ s} & \beta &= 3.5 \text{ km s}^{-1} \end{aligned} \quad (19)$$

for a fault surface $0 < \xi_1 < 10 \text{ km}$ (and of course $-\infty < \xi_2 < \infty$). The solutions in Figs 2–4 were computed at the point $\mathbf{x} = (0, 0, -5) \text{ km}$. As a check on the results we also show the displacement solutions computed for a long three-dimensional shear dislocation with parameters (19), but finite length ($0 < \xi_1 < 10 \text{ km}$; $-25 < \xi_2 < 25 \text{ km}$). The three-dimensional fault model is based on Haskell's 1969 paper.

Kanamori (1974, private communication) has corrected two errors in Haskell's (1969) paper. In the last line of equation (3.3), $\dot{D}(\xi_1, \xi_2, t - r/\beta)$ should be

$$\dot{D}_1(\xi_1, \xi_2, t - r/\beta).$$

In the first line of equation (4.3), $5\gamma_1^2$ should be $5\gamma_3^2$.

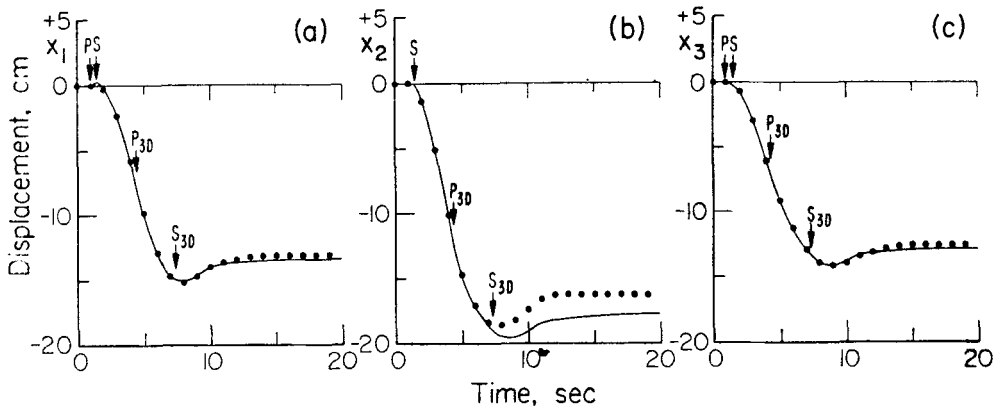


FIG. 2. Displacements computed at $\mathbf{x} = (0, 0, -5)$ for parameters (19).

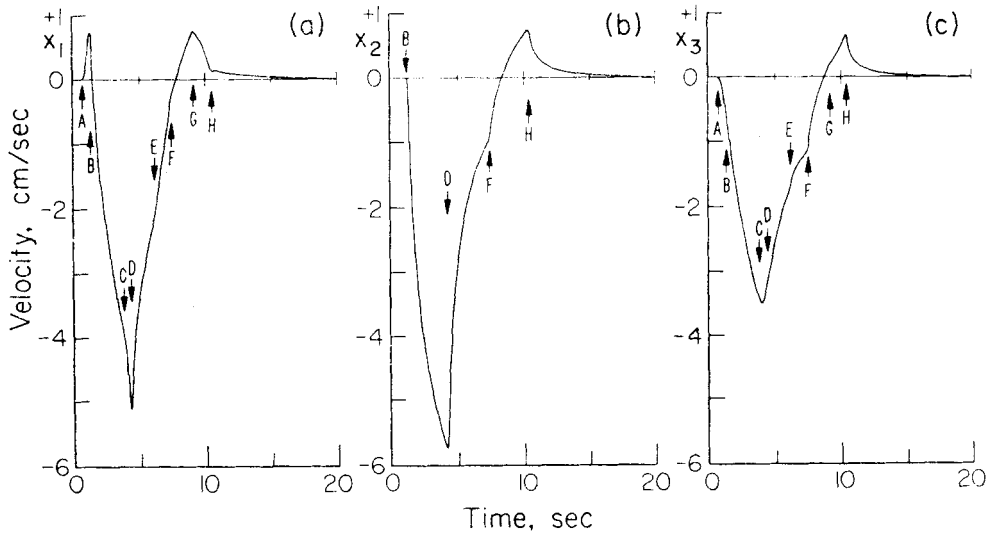


FIG. 3. Velocities computed at $\mathbf{x} = (0, 0, -5)$ for parameters (19)

The displacements from the two-dimensional model are plotted in Fig. 2 as continuous lines. Displacements from the three-dimensional model are plotted as dots. Both solutions are almost identical until the P arrival from the end of the three-dimensional fault (at $t = 4.25$ s). Major differences between the three-dimensional solutions and the two-dimensional solutions occur only after the S arrival from the end of the fault (at $t = 7.28$ s). Even in the worst case (the x_2 displacement) the final static values differ only by about 7 per cent. Note that first motion in the x_1 direction is positive until the S wave dominates.

Velocities (Fig. 3) and accelerations (Fig. 4) for the two-dimensional model were computed by difference operators. The letters used as labels in Figs 3 and 4 correspond to either starting or stopping of rupture directly 'below' and observation point; they are explained in more detail in Table 1. (The computed accelerations were smoothed to remove numerical noise caused by the fact that each of the labelled features is actually a $t^{-1/2}$ singularity. The singularity can be eliminated by convolving the accelerations with an accelerograph response.) Perhaps studies of simple models like the one in this paper may help in interpreting possible 'breakout' phases on strong motion records.

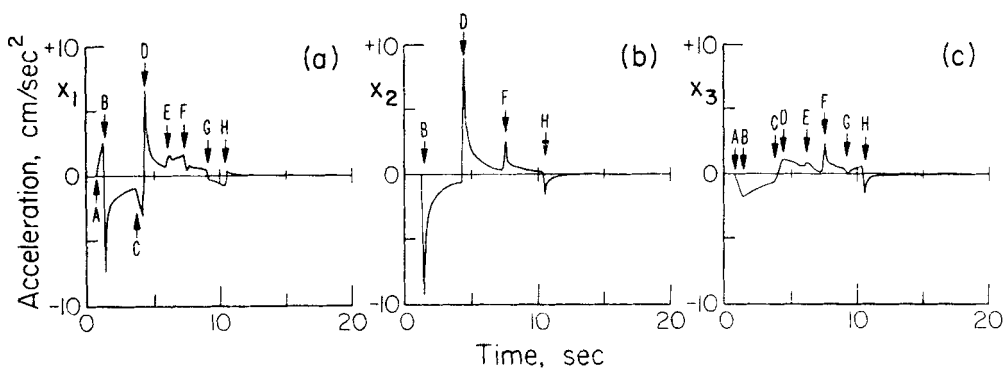


FIG. 4. Accelerations computed at $\mathbf{x} = (0, 0, -5)$ for parameters (19).

Table 1

Labels in Figs 3 and 4

Label	Time (s)	
A	·83	<i>P</i> arrival from rupture start (0, 0, 0)
B	1·43	<i>S</i> arrival from rupture start (0, 0, 0)
C	3·83	<i>P</i> arrival from rupture end (0, 0, 0)
D	4·43	<i>S</i> arrival from rupture end (0, 0, 0)
E	6·21	<i>P</i> arrival from rupture start (10, 0, 0)
F	7·54	<i>S</i> arrival from rupture start (10, 0, 0)
G	9·21	<i>P</i> arrival from rupture end (10, 0, 0)
H	10·54	<i>S</i> arrival from rupture end (10, 0, 0)

4. Conclusions

Analytic solutions for a two-dimensional shear dislocation with an arbitrary time function are given. The analytic solutions have been evaluated numerically for a propagating ramp source function.

Acknowledgment

Discussions with D. M. Cole, D. V. Helmberger, D. G. Harkrider, and H. Kanamori were most helpful. H. Kanamori kindly permitted my use of his three-dimensional dislocation program. My thanks to B. J. Sloan for typing the paper and L. Lenches for drafting the figures. This research was supported by the Advanced Research Projects Agency of the Department of Defence and was monitored by the Air Force Office of Scientific Research under Contract No. F44620-72-C-0078.

*Seismological Laboratory,
California Institute of Technology,
Pasadena, California 91109.*

References

- Churchill, R., 1958. *Operational mathematics*, McGraw-Hill, New York.
- de Hoop, A. T., 1958. *Representation theorems for the displacement in an elastic solid and their application to elastodynamic diffraction theory*, Thesis, Technische Hogeschool, Delft.
- Dix, C. H., 1954. The method of Cagniard in seismic pulse problems, *Geophysics*, **19**, 722-738.
- Haskell, N. A., 1964. Total energy and energy spectral density of elastic wave radiation from propagating faults, *Bull. seism. Soc. Am.*, **54**, 1811-1841.
- Haskell, N. A., 1969. Elastic displacements in the near-field of a propagating fault, *Bull. seism. Soc. Am.*, **59**, 865-908.
- Haskell, N. A. & Thomson, K. C., 1972. Elastodynamic near field of a finite, propagating tensile fault. *Bull. seism. Soc. Am.*, **62**, 675-697.
- Love, A. E. H., 1927. *A treatise on the mathematical theory of elasticity*, 4th ed., Dover, New York.
- Maruyama, T., 1963. On the force equivalents of dynamical elastic dislocations with reference to the earthquake mechanism, *Bull. earthq. Res. Inst., Tokyo Univ.*, **41**, 467-486.
- Niazy, A., 1973. Elastic displacements caused by a propagating crack in an infinite medium, *Bull. seism. Soc. Am.*, **63**, 357-379.
- Thomson, K. C. & Haskell, N. A., 1972. Elastodynamic near field of a finite propagating transverse shear fault, *J. geophys. Res.*, **77**, 2574-2582.